JOURNAL OF COMPUTATIONAL PHYSICS 20, 81–96 (1976)

On the Firehose Instability of Alfven Waves

YU. A. BEREZIN AND V. A. VSHIVKOV

Computing Center, Novosibirsk, U.S.S.R.

Received March 11, 1975; revised June 26, 1975

The firehose instability of Alfven waves in an anisotropic rarefied plasma is studied by analytical and effective numerical methods.

It is known that the Alfven waves propagating along the static magnetic field $\mathbf{H}_0$ direction in anisotropic high β plasmas are unstable when $p_\parallel > p_\perp + H_0^2/4\pi$, where $p_\parallel$ and $p_\perp$ are the plasma pressures parallel and perpendicular to the magnetic field, respectively [1, 2]. This criterion is defined by macroscopic parameters of the plasma; hence, it is natural to expect that the firehose instability will be described adequately by hydrodynamic-type equations. In such a consideration it must be assumed, of course, that characteristic wavelengths are much longer than the ion cyclotron radius ($KR \ll 1$); otherwise, any hydrodynamical model of plasmas fails.

Chew, Goldberger, and Low's (CGL) model [3] and the modifications accounting for the finite cyclotron radius (FCR) [4–6], are often used to describe rarefied anisotropic plasma. Sagdeev and Kennel [2] have considered the Alfven turbulence connected with destabilization of Alfven waves by the firehose instability as a shock dissipation mechanism for solar wind. Sagdeev and Berezin [7] have considered a nonlinear model of the instability with the FCR and found an analytical solution in the form of a monochromatic wave with circular polarization. Berezin [8] derived the equations for the case of small, but finite, amplitudes and showed that the solutions describing unstable Alfven waves are similar for plasmas with different parameters. To solve the firehose instability problem with general initial conditions is, at present, out of the question. This work is devoted to designing numerical methods for solving this problem.

1. FORMULATION

The equations for the transverse Alfven waves in the absence of longitudinal motion can be written as

$$\rho \frac{\partial u}{\partial t} + \frac{\partial}{\partial z}\left\{(p_\parallel - p_\perp)\frac{H_0 H_x}{H^2} - \frac{H_0 H_x}{4\pi} - \Omega^{-1}\left(p_\perp + \frac{p_\parallel - p_\perp}{H^2} H_0^2\right)\frac{\partial v}{\partial z}\right\} = 0$$

$$\rho \frac{\partial v}{\partial t} + \frac{\partial}{\partial z}\left\{(p_\parallel - p_\perp)\frac{H_0 H_y}{H^2} - \frac{H_0 H_y}{4\pi} + \Omega^{-1}\left(p_\perp + \frac{p_\parallel - p_\perp}{H^2} H_0^2\right)\frac{\partial u}{\partial z}\right\} = 0 \tag{1}$$

$$\frac{\partial H_x}{\partial t} = H_0 \frac{\partial u}{\partial z} \qquad \frac{\partial H_y}{\partial t} = H_0 \frac{\partial v}{\partial z}$$

$$\frac{\partial}{\partial t}(p_\parallel H^2) = 0 \qquad \frac{\partial}{\partial t}(p_\perp / H) = 0.$$

Here the axis Z is directed along the static magnetic field $\mathbf{H}_0$, where u, v are the x, y components of velocity, $H^2 = H_x^2 + H_y^2 + H_0^2$, $\rho = \text{const}$ is the plasma density, and $\Omega = eH_0/m_i c$, $R = \Omega^{-1}(p_\parallel/\rho)^{1/2}$ is the ion cyclotron radius. The terms connected with Ω^{-1} describe the magnetic viscosity.

If our problem is considered as a periodic one with period L, then we can obtain the following conservation law

$$\int_0^L (\rho(u^2 + v^2)/2 + (1/2)\, p_\parallel + p_\perp + H^2/8\pi)\, dz \equiv \int_0^L Q(z, t)\, dz = \text{const}.$$

The density of total energy $Q(z, t)$, consists of densities of kinetic $\rho((u^2 + v^2)/2)$, internal $(1/2)\, p_\parallel + p_\perp$, and magnetic $H_0^2/8\pi$ energy. In an isotropic gas, the density of internal energy is defined as $\epsilon = p/(\gamma - 1)$, $\gamma = (m + 2)/m$, where m is the number of degrees of freedom. In the case of an anisotropic plasma, the motion of particles along the magnetic field can be considered as one-dimensional with $m = 1, \gamma = 3$ and that perpendicular to the magnetic field as two-dimensional with $m = 2$, $\gamma = 2$. Therefore, the internal energy per unit mass connected with longitudinal motion is equal to $p_\parallel/2$ and with transverse motion $p_\perp$.

Linear analysis yields

$$\omega_K = \omega^{(K)} + i\gamma_K,$$
$$\omega^{(K)} = \Omega K^2 R^2/2,$$
$$\gamma_K = K((\Delta p - (1/4)\, p_\parallel K^2 R^2)/\rho)^{1/2},$$

where $\Delta p = p_\parallel - p_\perp - H_0^2/4\pi$ is the degree of plasma anisotropy. We show that the Alfven waves of small amplitudes are unstable when

$$p_\parallel > p_\perp + H_0^2/4\pi,$$
$$KR < 2(\Delta p/p_\parallel)^{1/2}.$$

Since the hydrodynamical approach is valid for waves with $KR \ll 1$, the firehose instability can be described by hydrodynamic-type equations when the plasma anisotropy is small ($\Delta p \ll p_\parallel$).

It has been shown [8] that for waves of small but finite amplitudes, the model set of equations

$$\begin{aligned} &\frac{\partial u}{\partial t} + \frac{\partial}{\partial z}\left[(1 - H_\perp{}^2)H - \frac{\partial v}{\partial z}\right] = 0 \\ &\frac{\partial v}{\partial t} + \frac{\partial}{\partial z}\left[(1 - H_\perp{}^2)B + \frac{\partial u}{\partial z}\right] = 0 \\ &\frac{\partial H}{\partial t} = \frac{\partial u}{\partial z} \qquad \frac{\partial B}{\partial t} = \frac{\partial v}{\partial z} \qquad H_\perp{}^2 = H^2 + B^2 \end{aligned} \tag{2}$$

can be derived by transforming to new variables

$$\begin{aligned} t' = \frac{\Omega\, \Delta p}{p_\parallel}\, t, \qquad z' = \frac{\Omega}{p_\parallel}\,(\rho\, \Delta p)^{1/2}\, z, \\ u', v' = (1/\Delta p)(\rho(2p_\parallel - p_\perp/2))^{1/2}\, u, v, \\ H', B' = ((2p_\parallel - p_\perp/2)/\Delta p)^{1/2}\, H, B, \\ H = H_x/H_0\,, \qquad B = H_y/H_0 \end{aligned}$$

(primes have been omitted).

Equations (2) do not contain any parameters of the plasma state ($p_\parallel$, $p_\perp$, H_0), and all solutions for different $p_\parallel$, $p_\perp$, H_0 will be similar. The set (2) is a very interesting one from a mathematical point of view.

If the problem is periodic with period L, then we can write the following conservation law:

$$\begin{aligned} &\int_0^L Q_1(z, t)\, dz = \int_0^L Q_1(z, 0)\, dz, \\ &Q_1 = (u^2 + v^2)/2 + (H^2 + B^2 - 1)^2/4 \end{aligned} \tag{3}$$

2. Study of Model Equations

Any stationary solution of the set (2) has the form $f \equiv (u, v, H, B) = f_1 = \text{const}$. Linear analysis yields

$$\omega_K = (1/2)\, K^4 - (1 - 2\mathscr{D}^2 \mp ((\mathscr{D}^2 + K^2)^2 - (1 + 3K^2/4)\, K^2)^{1/2})\, K^2,$$
$$\mathscr{D}^2 = H_1{}^2 + B_1{}^2,$$

and it is necessary for reality of ω_K (that is, for stability of the waves with wavenumber K) to have

$$\begin{aligned} (\mathscr{D}^2 + K^2)^2 - (1 - 3K^2/4)\, K^2 \geqslant 0 \\ K^2/2 - 1 + 2\mathscr{D}^2 \geqslant 0 \\ 1 - 4\mathscr{D}^2 + 3\mathscr{D}^4 \geqslant 0. \end{aligned}$$

The results of analysis of these conditions are represented in Fig. 1, where the dashed line shows the region of stability. When $\mathscr{D}^2 = 1$, the disturbances of any wavelength are stable. The other region of stability is limited by a part of the curve $9(K^2 + 2/3)^2 - 12(\mathscr{D}^2 + K^2)^2 = 4$ between the points $(2, 0)$, $((2/3)^{1/2}, 1/3)$, and a part of the line $\mathscr{D} = 1/3^{1/2}$. In Fig. 2 the dependence of γ_K on the wavenumber K for different values of the transverse magnetic field $0 \leqslant \mathscr{D} \leqslant 1/3^{1/2}$ is represented.

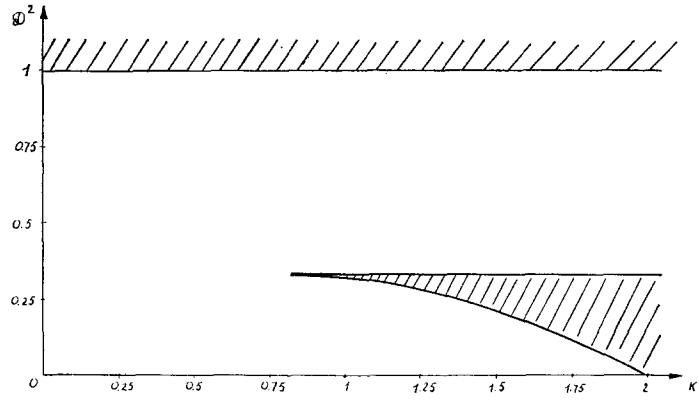

FIGURE 1

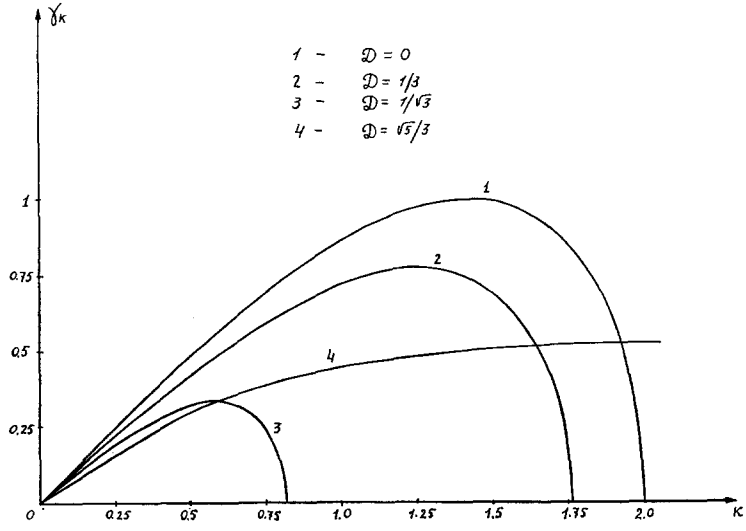

FIGURE 2

The regions of instability and maximum increment decrease with an increasing value of $\mathscr{D}$. In the case of propagation along the magnetic field ($\mathscr{D} = 0$), we have $\gamma_K = K(1 - K^2/4)^{1/2}$. When $\mathscr{D} = 1/3^{1/2}$, we have $\gamma_K = K(2/3 - K^2)^{1/2}$ and $\gamma = \gamma_{\max} = 1/3$ at $K = 1/3^{1/2}$. In the region $1/3 < \mathscr{D}^2 < 1$, all the waves are unstable.

According to [7, 8], sets (1) and (2) have partial analytical solutions:

$$\begin{aligned} H(z, t) &= A(t) \sin(Kz + \varphi(t)) \\ B(z, t) &= A(t) \cos(Kz + \varphi(t)) \\ u(z, t) &= (1/K)[A\dot{\varphi} \sin(Kz + \varphi(t)) - \dot{A} \cos(Kz + \varphi(t))] \\ v(z, t) &= (1/K)[\dot{A} \sin(Kz + \varphi(t)) + A\dot{\varphi} \cos(Kz + \varphi(t))]. \end{aligned} \tag{4}$$

In the case of the model set (2), we have the following equations for the amplitude $A(t)$ and phase $\varphi(t)$:

$$\begin{aligned} \dot{A}^2 + U(A) &= E = \text{const} \\ \dot{\varphi}(t) &= -(1/2)\, K^2 + C/A^2(t) \\ U(A) &= (1/2)\, K^2A^2(A^2 + (1/2)\, K^2 - 2) + C^2/A^2 \\ E &= \dot{A}_0^2 + (1/2)\, K^2A_0^2(A_0^2 + (1/2)\, K^2 - 2) + C^2/A_0^2 \\ C &= A_0^2(\dot{\varphi}(0) + (1/2)\, K^2), \end{aligned} \tag{5}$$

where A_0 is an initial amplitude, $\dot{A}_0 = (dA/dt)|_{t=0}$. The case $C = 0$ and $\varphi(t) = -K^2t/2$ have been considered in [8]. The functions $U(A)$ at different values of C and $K = 2^{1/2}$ are represented in Fig. 3, from which one can conclude that the amplitude of the wave (4) changes periodically with time. If the initial conditions A_0, $\dot{A}_0$, $\dot{\varphi}(0)$ are given, minimum $A_{\min}$ and maximum $A_{\max}$ can be determined from the equation $U(A_{\text{extr}}) = E$. In Fig. 4, the dependence of $A_{\min}$, $A_{\max}$ on C and E is represented ($K = 2^{1/2}$). The maximum amplitude increases together with the value of C (given the initial amplitude A_0, the growth of the value of C means the growth of the initial wave frequency $\dot{\varphi}(0)$). When $C \gg 1$, one can obtain the following asymptotic relation: $A_{\max} \sim C^{1/2}$. The solution of the set (5) with the initial conditions

$$\begin{aligned} u(z, 0) &= (1/K)(A_0\dot{\varphi}_0 \sin Kz - \dot{A}_0 \cos Kz) \\ v(z, 0) &= (1/K)(A_0\dot{\varphi}_0 \cos Kz + \dot{A}_0 \sin Kz) \\ H(z, 0) &= A_0 \sin Kz \qquad B(z, 0) = A_0 \cos Kz \end{aligned} \tag{6}$$

can be expressed by elliptic functions and analyzed qualitatively. However, for a quantitive description of the solution, it was easier to use some numerical, high-accuracy method (for example, Runge–Kutta's or Adams') which showed the coincidence of the solutions obtained by calculation of the elliptic functions and

those by Runge–Kutta's method. As follows from Table II, the integration step $\tau = 10^{-2}$ is sufficient for the definition of even the most quickly increasing solution with $\gamma_k = \gamma_{\max}$ $(k = 2^{1/2})$ since decreasing the steps fivefold does not lead to changes of the solution.

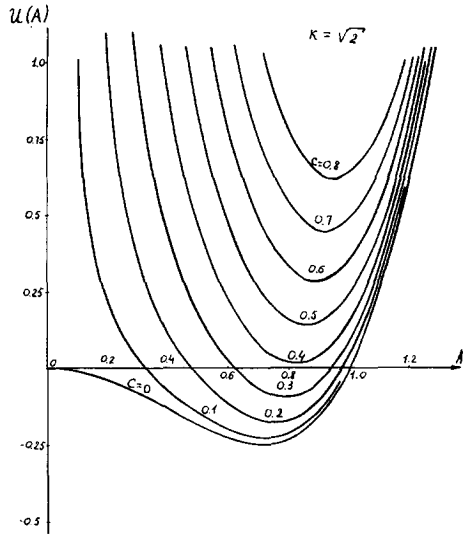

FIGURE 3

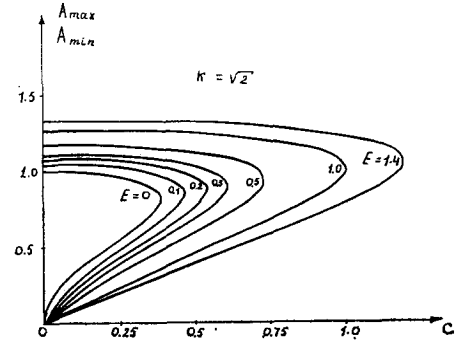

FIGURE 4

Figure 5 shows such solutions for $C = 0$ and $C = 0.1$. As mentioned earlier, numerical methods must be used for the solution of (2) with arbitrary initial conditions. We shall use the solutions (Fig. 5) for a comparison of the finite-difference schemes, as described below.

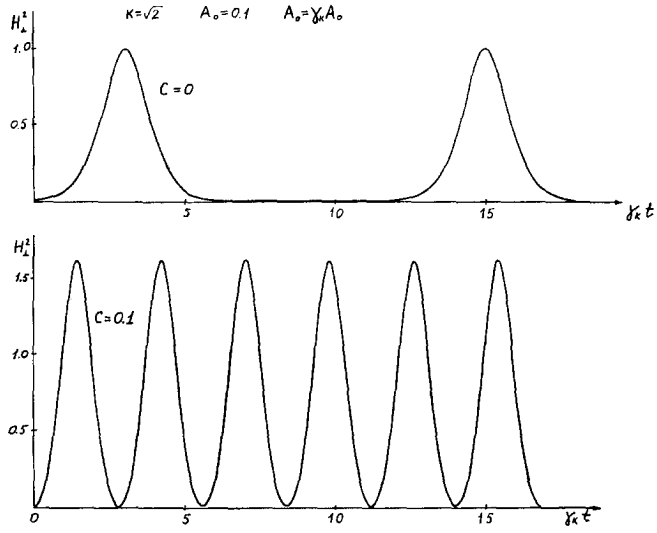

FIGURE 5

3. NUMERICAL METHODS FOR THE MODEL SET

For the sake of convenience we repeat the formulation of the problem. It is necessary to find a solution of the set (2) in the region $\{0 \leqslant z \leqslant L, 0 \leqslant t \leqslant T\}$ satisfying the periodic boundary conditions

$$f(0, t) = f(L, t) \tag{7}$$

and the more or less arbitrary initial conditions

$$f(z, 0) = f^0(z).$$

(1) *Spectral Method*

Let us choose as a basis the complete set of functions $\exp(im\omega z)$, $\omega = 2\pi/L$, $m = 0, \pm 1, \pm 2, \ldots$ satisfying the boundary conditions (7). Using Fourier transformation for the space coordinate z, we obtain the following system of ordinary nonlinear equations

$$\begin{aligned}
(du_m/dt) &= -i\omega m H_m + \omega^2 m^2 v_m + i\omega m \sum_{n+n'+n''=m} H_n(H_{n'}H_{n''} + B_{n'}B_{n''}) \\
(dv_m/dt) &= -i\omega m B_m - \omega^2 m^2 u_m + i\omega m \sum_{n+n'+n''=m} B_n(H_{n'}H_{n''} + B_{n'}B_{n''}) \\
(dH_m/dt) &= i\omega m u_m \\
(dB_m/dt) &= i\omega m v_m
\end{aligned} \tag{8}$$

with the initial conditions

$$f^0(z) = \sum_{m=-\infty}^{\infty} f_m(0) \exp(im\omega z).$$

In order to solve Eqs. (8) with a finite number of harmonics $|m| < N$, one may use any method of high accuracy, for example, Runge–Kutta's or Adams'. However, there is the difficulty that a direct evaluation of the sums

$$R_m = \sum_{|n|<N} \sum_{|n'|<N} \sum_{|n''|<N} A_n B_{n'} C_{n''}, \qquad n + n' + n'' = m$$

is too inefficient. We have made a generalization of Orszag's method for double nonlocal sums [9] and obtained the following formula:

(a) Fourier transformation of the values H_m, B_m:

$$\hat{h}(j) = \sum_{m=-N}^{N-1} H_m e^{imx_j} \qquad \hat{b}(j) = \sum_{m=-N}^{N-1} B_m e^{imx_j}$$

$$\tilde{h}(j) = \sum_{m=-N}^{N-1} H_m e^{imx_{j+1/3}} \qquad \tilde{b}(j) = \sum_{m=-N}^{N-1} B_m e^{imx_{j+1/3}}$$

$$\bar{h}(j) = \sum_{m=-N}^{N-1} H_m e^{imx_{j+2/3}} \qquad \bar{b}(j) = \sum_{m=-N}^{N-1} B_m e^{imx_{j+2/3}},$$

where

$$H_{-N} = B_{-N} = 0, \qquad x_j = \pi j/N, \qquad x_{j+1/3} = \pi(j + 1/3)/N,$$
$$x_{j+2/3} = \pi(j + 2/3)/N, \qquad j = 0, 1, \ldots, 2N - 1,$$

(b) Multiplication:

$$\hat{p}(j) = \hat{h}(j)(\hat{h}^2(j) + \hat{b}^2(j)) \qquad \hat{q}(j) = \hat{b}(j)(\hat{h}^2(j) + \hat{b}^2(j))$$
$$\tilde{p}(j) = \tilde{h}(j)(\tilde{h}^2(j) + \tilde{b}^2(j)) \qquad \tilde{q}(j) = \tilde{b}(j)(\tilde{h}^2(j) + \tilde{b}^2(j))$$
$$\bar{p}(j) = \bar{h}(j)(\bar{h}^2(j) + \bar{b}^2(j)) \qquad \bar{q}(j) = \bar{b}(j)(\bar{h}^2(j) + \bar{b}^2(j)).$$

(c) Inverse Fourier transformation:

$$\hat{P}_m = \frac{1}{2N} \sum_{j=0}^{2N-1} \hat{p}(j)\, e^{-imx_j} \qquad \hat{Q}_m = \frac{1}{2N} \sum_{j=0}^{2N-1} \hat{q}(j)\, e^{-imx_j},$$

the expressions $\tilde{P}_m$, $\tilde{Q}_m$, $\bar{P}_m$, and $\bar{Q}_m$ are defined similarly.

(d) Evaluation of the triple sums:

$$P_m = \tfrac{1}{3}[\hat{P}_m + e^{-i(\pi m/(3N))}\tilde{P}_m + e^{-i(2\pi m/(3N))}\bar{P}_m]$$
$$Q_m = \tfrac{1}{3}[\hat{Q}_m + e^{-i(\pi m/(3N))}\tilde{Q}_m + e^{-i(2\pi m/(3N))}\bar{Q}_m],$$

where

$$P_m = \sum_{|n|<N} \sum_{\substack{|n'|<N \\ n+n'+n''=m}} \sum_{|n''|<N} H_n(H_{n'}H_{n''} + B_{n'}B_{n''})$$

$$Q_m = \sum_{|n|<N} \sum_{\substack{|n'|<N \\ n+n'+n''=m}} \sum_{|n''|<N} B_n(H_{n'}H_{n''} + B_{n'}B_{n''}).$$

In the algorithm just considered, it is necessary to compute the values

$$\hat{a}(j) = \sum_{m=-N}^{N-1} A_m w^{jm},$$

$w = \exp(i\pi/N)$, and $j = 0, 1, \ldots, 2N - 1$, for which one must make $4N^2$ multiplications. The number can be reduced if one uses the fast Fourier transform algorithm [10]. In our case, choosing $N = 2^r$, we obtain $16N(3r + 5)$ multiplications for computing P_m, Q_m, instead of $4(2N - 1)^2$ multiplications at the direct calculations P_m, Q_m.

(2) *Finite-Difference Schemes*

In order to choose the best difference scheme for solving the problem (2), (6) we have made a comparison of some schemes according to the following characteristics: instability region, values of growth rates, energy conservation, and deviation from the exact solution.

(a) Explicit scheme with accuracy $0(\tau, h^2)$.

$$u_j^{n+1} = u_j^n - \tau\{\Lambda_1(aH)_j^n - \Lambda_{11}v_j^n\}$$
$$v_j^{n+1} = v_j^n - \tau\{\Lambda_1(aB)_j^n + \Lambda_{11}u_j^{n+1}\}$$
$$H_{j+1/2}^{n+1} = H_{j+1/2}^n + \tau\Lambda_1 u_{j+1/2}^{n+1}$$
$$B_{j+1/2}^{n+1} = B_{j+1/2}^n + \tau\Lambda_1 v_{j+1/2}^{n+1},$$

where

$$a = 1 - H^2 - B^2, \qquad \Lambda_1 f_j = h^{-1}(f_{j+1/2} - f_{j-1/2}),$$
$$\Lambda_{11}f_j = h^{-2}(f_{j+1} - 2f_j + f_{j-1}), \qquad j = 0, 1, \ldots, N.$$

This scheme is similar to that described in [11] for the linear equation of elastic vibrations.

(b) Implicit scheme with accuracy $0(\tau, h^2)$.

$$u_j^{n+1} = u_j^n - \tau\{\Lambda_1(a^n H^{n+1})_j - \Lambda_{11} v_j^{n+1}\}$$

$$v_j^{n+1} = v_j^n - \tau\{\Lambda_1(a^n B^{n+1})_j + \Lambda_{11} u_j^{n+1}\}$$

$$H_{j+1/2}^{n+1} = H_{j+1/2}^n + \tau\Lambda_1 u_{j+1/2}^{n+1}$$

$$B_{j+1/2}^{n+1} = B_{j+1/2}^n + \tau\Lambda_1 v_{j+1/2}^{n+1}.$$

This scheme may be realized by cyclic matrix sweeping.

(c) Predictor–corrector I with accuracy $0(\tau^2, h^2)$.

$$u_j^{n+1/2} = u_j^n - \frac{\tau}{2}\{\Lambda_1(a^n H^{n+1/2})_j - \Lambda_{11} v_j^{n+1/2}\}$$

$$v_j^{n+1/2} = v_j^n - \frac{\tau}{2}\{\Lambda_1(a^n B^{n+1/2})_j + \Lambda_{11} u_j^{n+1/2}\}$$

$$H_{j+1/2}^{n+1/2} = H_{j+1/2}^n + \frac{\tau}{2}\Lambda_1 u_{j+1/2}^{n+1/2}$$

$$B_{j+1/2}^{n+1/2} = B_{j+1/2}^n + \frac{\tau}{2}\Lambda_1 v_{j+1/2}^{n+1/2}$$

$$u_j^{n+1} = u_j^n - \tau\{\Lambda_1(aH)_j^{n+1/2} - \Lambda_{11} v_j^{n+1/2}\}$$

$$v_j^{n+1} = v_j^n - \tau\{\Lambda_1(aB)_j^{n+1/2} + \Lambda_{11} u_j^{n+1/2}\}$$

$$H_{j+1/2}^{n+1} = H_{j+1/2}^n + \tau\Lambda_1 u_{j+1/2}^{n+1/2}$$

$$B_{j+1/2}^{n+1} = B_{j+1/2}^n + \tau\Lambda_1 v_{j+1/2}^{n+1/2}.$$

(d) Predictor–corrector II with accuracy $0(\tau^2, h^2)$. This scheme is a modification of scheme (c) with the same predictor and the following corrector:

$$u_j^{n+1} = u_j^n - \tau\left\{\Lambda_1\left(\frac{a^{n+1} + a^n}{2} H^{n+1/2}\right)_j - \Lambda_{11} v_j^{n+1/2}\right\}$$

$$v_j^{n+1} = v_j^n - \tau\left\{\Lambda_1\left(\frac{a^{n+1} + a^n}{2} B^{n+1/2}\right)_j + \Lambda_{11} u_j^{n+1/2}\right\}$$

$$H_{j+1/2}^{n+1} = H_{j+1/2}^n + \tau\Lambda_1 u_{j+1/2}^{n+1/2}$$

$$B_{j+1/2}^{n+1} = B_{j+1/2}^n + \tau\Lambda_1 v_{j+1/2}^{n+1/2}.$$

(e) Iterative scheme.

$$u_j^{n+1/2,s+1} = u_j^n - \frac{\tau}{2}\left\{\Lambda_1\left(\frac{a^{n+1,s}+a^n}{2}H^{n+1/2,s+1}\right)_j - \Lambda_{11}v_j^{n+1/2,s+1}\right\}$$

$$v_j^{n+1/2,s+1} = v_j^n - \frac{\tau}{2}\left\{\Lambda_1\left(\frac{a^{n+1,s}+a^n}{2}B^{n+1/2,s+1}\right)_j + \Lambda_{11}u_j^{n+1/2,s+1}\right\}$$

$$H_{j+1/2}^{n+1/2,s+1} = H_{j+1/2}^n + \frac{\tau}{2}\Lambda_1 u_{j+1/2}^{n+1/2,s+1}$$

$$B_{j+1/2}^{n+1/2,s+1} = B_{j+1/2}^n + \frac{\tau}{2}\Lambda_1 v_{j+1/2}^{n+1/2,s+1}$$

$$u_j^{n+1,s+1} = 2u_j^{n+1/2,s+1} - u_j^n$$

$$v_j^{n+1,s+1} = 2v_j^{n+1/2,s+1} - v_j^n$$

and the same for the functions $H_{j+1/2}^{n+1,s+1}$, $B_{j+1/2}^{n+1,s+1}$. Here s is the iteration number $f^{n+1,0} = f^n$.

(3) *Finite-Difference Instability Regions and Growth Rates*

Linear analysis of the schemes described above yields the following expressions for the growth rates:

(a) Explicit scheme.

$$\gamma_K^{(1)}(\tau, h) = \kappa(1 - \kappa^2/4)^{1/2}\,[1 + \kappa^2(\kappa^2 - 1)\,\tau^2/24].$$

(b) Implicit scheme.

$$\gamma_K^{(2)}(\tau, h) = \kappa(1 - \kappa^2/4)^{1/2} + \kappa^2(1 - \kappa^2/2)\,\tau/2$$

(c) Predictor–corrector and iterative schemes.

$$\gamma_K^{(3)}(\tau, h) = \kappa(1 - \kappa^2/4)^{1/2}\,[1 - \kappa^2(\kappa^2 - 1)\,\tau^2/12],$$

where $\kappa = (2/h)\sin(Kh/2)$.

In Table I the values of the finite-difference and differential growth rates are represented by ($\tau = 10^{-2}$, $h = 0.11$). The best scheme is an iterative one.

TABLE I

k	0.2	0.4	0.6	0.8	1.0	1.2	1.4	1.6	1.8
γ_k	0.198997	0.391918	0.572364	0.733212	0.866025	0.960000	0.999800	0.960000	0.784602
$\gamma_k^{(1)}(\tau, h)$	0.198993	0.391887	0.572268	0.733016	0.865729	0.959691	0.999766	0.960991	0.788854
$\gamma_k^{(2)}(\tau, h)$	0.199190	0.392625	0.573748	0.735198	0.868228	0.961689	0.999910	0.957315	0.778717
$\gamma_k^{(3)}(\tau, h)$	0.198994	0.391888	0.572269	0.733018	0.865729	0.959684	0.999743	0.960943	0.788783

TABLE II

	t	2	4	6	8	10
Runge–Kutta method	$\tau = 10^{-2}$	0.426001	0.413949	0.963017×10^{-2}	0.131606×10^{-3}	0.144853×10^{-3}
	$\tau = 2 \times 10^{-3}$	0.426001	0.413949	0.963017×10^{-2}	0.131606×10^{-3}	0.144853×10^{-3}
Explicit	$\tau = 5 \times 10^{-3}$	0.425856	0.415831	0.972158×10^{-2}	0.152817×10^{-2}	0.726569×10^{-1}
Implicit	$\tau = 5 \times 10^{-3}$	0.425384	0.418219	0.138514×10^{-1}	0.679878×10^{-1}	0.991412
Predictor–Corrector I	$\tau = 10^{-2}$	0.425848	0.415867	0.969392×10^{-2}	0.141967×10^{-3}	0.498888×10^{-4}
Predictor–Corrector II	$\tau = 10^{-2}$	0.425843	0.415851	0.969337×10^{-2}	0.141783×10^{-3}	0.914817×10^{-4}
Iterative	$\tau = 10^{-2}$	0.425831	0.415914	0.969562×10^{-2}	0.141830×10^{-3}	0.914229×10^{-4}

(4) *Comparison with the Exact Solution and Energy Conservation.*

We consider the solution of Eqs. (5) obtained by fourth-order Runge–Kutta's or Adams' method as an "exact" solution. With our difference schemes, we obtain the numerical solution of Eqs. (2) with initial conditions (6) and make a comparison of the average square magnetic field:

$$\langle H_\perp{}^2(t^n)\rangle = N^{-1}\sum_{j=1}^{N}[(H_j{}^n)^2 + (B_j{}^n)^2]$$

with the value $A^2(t^n) = H^2(t^n) + B^2(t^n)$. In Table II the time dependence of the values $A^2(t)$ and $\langle H_\perp{}^2(t)\rangle$ for the case of $K = 2^{1/2}$, $A_0 = 0.1$, $\dot{\varphi}(0) = -K^2/2$ is represented. For the explicit and implicit schemes the time step was $\tau = 5 \times 10^{-3}$; for the predictor–corrector and iterative schemes the step was $\tau = 10^{-3}$; the space mesh was $h = 0.11$; the iterative parameter was $\epsilon = 10^{-5}$. Explicit and implicit schemes reproduce the exact solution for approximately a half-period of $A^2(t)$. After that, the numerical solution does not coincide with the exact solution. This effect is connected with the nonsymmetric explicit scheme. As the computations show, predictor–corrector and iterative schemes reproduce the exact solution very well.

The finite-difference analog of energy (3) has the following form

$$W^n = h\sum_{j=1}^{N}\{\tfrac{1}{2}[(u_j{}^n)^2 + (v_j{}^n)^2] + \tfrac{1}{4}[1 - (H_{j+1/2}^n)^2 - (B_{j+1/2}^n)^2]^2\}.$$

After some algebra we obtain $(W^{n+1} - W^n)/\tau = 0(\tau)$, for the explicit and implicit schemes;

$(W^{n+1} - W^n)/\tau = 0(\tau^2)$, for the predictor–corrector scheme, and $W^{n+1} = W^n$, for the iterative scheme (when we have a convergence of iterations).

In Table III the energy change

$$\delta W(t^n) = (W(t^n) - W(0))/W(0)$$

is given (the parameters were given earlier).

TABLE III

Schemes	$T = 2$	$T = 4$	$T = 6$	$T = 8$	$T = 10$
Explicit	0.235	0.245	0.177	0.161	0.200
Implicit	0.505	0.513	0.517	0.520	0.522
Predictor–Corrector I	0.136×10^{-2}	0.286×10^{-2}	0.485×10^{-2}	0.628×10^{-2}	0.702×10^{-2}
Predictor–Corrector II	0.322×10^{-3}	0.541×10^{-3}	0.371×10^{-3}	0.411×10^{-3}	0.988×10^{-3}
Iterative	0.399×10^{-7}	0.314×10^{-7}	0.167×10^{-7}	0.500×10^{-8}	0.361×10^{-7}

(5) *Comparison of Spectral and Finite Difference Methods*

For the comparison mentioned above, the calculations were made by both spectral and iterative methods. Optimization of the spectral method (with fast Fourier transformation) decreases the number of operations needed, even in a case of few harmonics, e.g., with $N = 2^5$ harmonics we have a gain of 1.5. The use of the Adams method for the solution of Eqs. (8) reduces the number of operations four fold as compared to the Runge–Kutta method. But even in this case, the iterative-difference scheme is faster for the same accuracy.

4. Some Results of Calculations

With an iterative scheme, we have examined the temporal evolution both of individual harmonics and their random sets with small initial amplitudes. If at the moment $t = 0$, the amplitudes of all the harmonics with the numbers $m \neq m_1$ are equal to zero, and the initial functions $(u, v, H, B)_{m_1}$ are arbitrary, then the energy of the harmonic with a number m_1 is transfered into the harmonics with numbers $m = \pm(21 + 1)\, m_1$, where $l = 0, 1, \ldots$. If the conditions in (6) are chosen as the initial conditions, energy remains only in the harmonic with the number m_1. The maximum transverse magnetic field in such a wave is equal to $(H_\perp)_{\max} = (2 - K^2/2)^{1/2}$ and the kinetic energy is equal to $K = \frac{1}{2}H_\perp{}^2(1 - \frac{1}{2}H_\perp{}^2)$. If at the initial moment $t = 0$ the amplitudes of the harmonics with the numbers $m_1, m_2, \ldots, m_l$ are nonzero, then the energy of these harmonics is transferred into all harmonics with the numbers nm_0, where m_0 is the greatest common divisor of the numbers $m_1, m_2, \ldots, m_l$, and $n = \pm 1, \pm 2, \ldots$. Gradually, this energy is redistributed over the same harmonics. Let a random distribution of all the functions u, v, H, B be given at the initial time. During a small time interval, amplitudes of the waves corresponding to the wavenumbers K from the domain of instability will grow proportionally to $\exp(\gamma_K t)$. When amplitudes of the harmonics become large

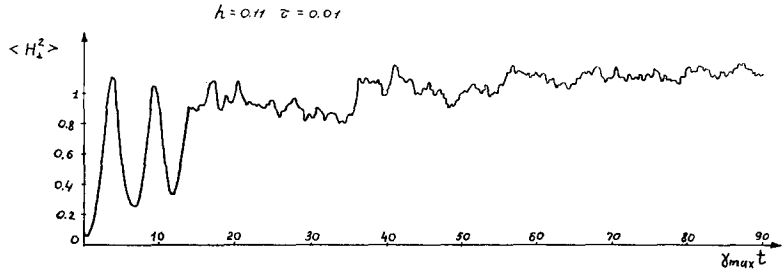

FIGURE 6

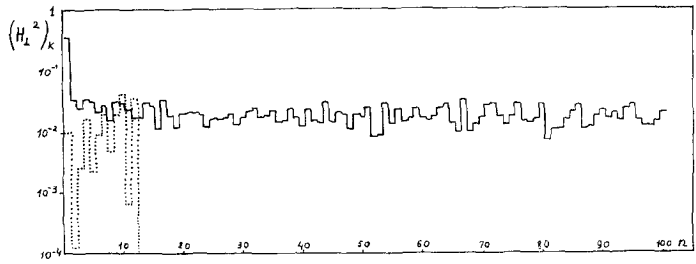

FIGURE 7

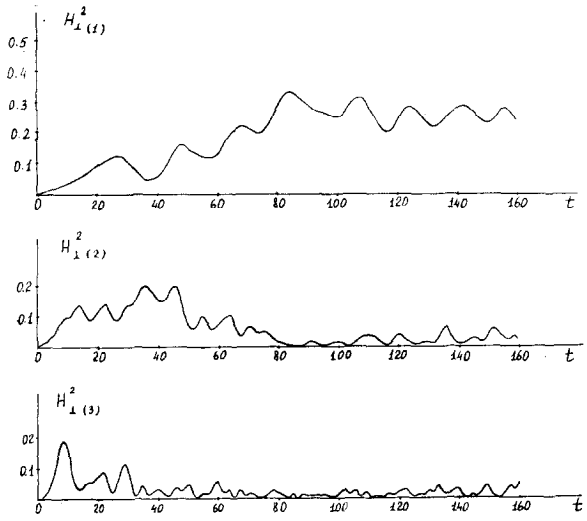

FIGURE 8

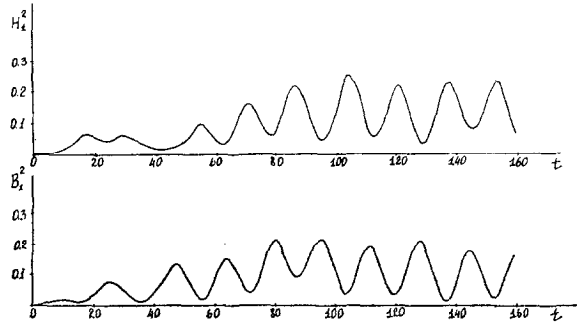

FIGURE 9

enough, the nonlinear interaction between them begins and as a result, a quasi-stationary regime is gradually reached. The mean square of the transverse magnetic field $\langle H_\perp{}^2 \rangle$ has random oscillations near some level, which does not depend on the distribution of the given initial energy over the harmonics. In Fig. 6, the temporal evolution of the mean square of the transverse magnetic field is represented; one can see that the level is reached after time $t \approx 20\gamma_{\max}^{-1}$. In Fig. 7, the distribution of the magnetic field energy density over the harmonics is represented (the dotted line represents the distribution at the initial moment and the solid line is for the distribution at $t = 100\gamma_{\max}^{-1}$). The calculations indicate that after some finite time the first harmonic with maximum wavelength has maximum energy; the remaining harmonics have energies about 10^{-1} as large as the energy of the first harmonic. In Fig. 8, the temporal evolution of the magnetic energy of the first harmonic with the wavenumbers $K = 0.283$, 0.566, 0.844 is represented. At the initial stage the energy of the third harmonic grows more rapidly, since it has the larger linear increment. Then, due to nonlinear interaction, the main part of the energy is gradually transferred, first to the second harmonic with $K = 0.566$, and later to the first one with $K = 0.283$. Fig. 9 represents the temporal evolution of $H_1{}^2$, $B_1{}^2$ for the first harmonic. After some transition time (≈ 40 to $50\gamma_{\max}^{-1}$), the values periodically change.

6. References

1. A. A. Vedenov, E. P. Velikhov, R. Z. Sagdeev, *Nucl. Fusion* **1** (1961), 83.
2. C. F. Kennel and R. Z. Sagdeev, *J. Geophys. Res.* **72** (1967), 3303.
3. G. F. Chew, M. L. Goldberger, and F. E. Low, *Proc. Roy. Soc. Ser. A.* **236** (1956), 112.
4. K. V. Roberts and J. B. Taylor, *Phys. Rev. Letters* **8** (1962), 197.
5. G. M. Zaslavskii and S. S. Moiseev, *Dokl. Acad. Nauk.* **6** (1962), 119.
6. C. F. Kennel and R. Z. Sagdeev, *J. Geophys. Res.* **72** (1967), 3327.
7. Yu. A. Berezin and R. Z. Sagdeev, *Sov. Phys. Dokl.* **14** (1969), 62.
8. Yu. A. Berezin, *Sov. Phys. JETP.* **34** (1972), 998.
9. S. A. Orszag, *Stud. Appl. Math.* **50** (1971), 293.
10. J. W. Cooley and J. W. Tukey, *Math. Comp.* **19** (1965), 297.
11. R. D. Richtmyer and K. W. Morton, "Difference Methods for Initial-Value Problems," Wiley, New York, 1967.